Journal of Science: Advanced Materials and Devices 5 (2020) 185–191

Contents lists available at ScienceDirect

Journal of Science: Advanced Materials and Devices

journal homepage: www.elsevier.com/locate/jsamd

Original Article

Fabrication and characterization of green synthesized ZnO nanoparticle based dye-sensitized solar cells

R. Shashanka [a, *], Halil Esgin [b], Volkan Murat Yilmaz [c], Yasemin Caglar [d]

[a] Department of Metallurgical and Materials Engineering, Bartin University, Bartin, 74100, Turkey
[b] Central Research Laboratory, Cukurova University, Adana, 01330, Turkey
[c] Central Research Laboratory, Bartin University, Bartin, 74100, Turkey
[d] Department of Physics, Faculty of Science, Eskisehir Technical University, Yunusemre Campus, Eskisehir, 26470, Turkey

ARTICLE INFO

Article history:
Received 10 March 2020
Received in revised form
12 April 2020
Accepted 16 April 2020
Available online 25 April 2020

Keywords:
ZnO nanoparticles
Tilia tomentosa
Green synthesis
Dye-sensitized solar cell
Bandgap

ABSTRACT

In the present study, we report on the synthesis of ZnO nanoparticles using *Tilia Tomentosa* (Ihlamur) leaves extract followed by calcination at 400 °C for 15 min. The prepared ZnO nanoparticles were characterized by XRD and SEM to study the phase and microstructure, respectively. The XRD analysis showed the absence of impurity peaks and the SEM image confirmed the spherical nature of the prepared ZnO nanoparticles with an average particle size of 80 nm. UV-Visible spectroscopy was used to study the optical properties, and the bandgap was calculated to be 3.55 eV. This large bandgap is attributed to the property of the semiconductor, which can be explored for solar cell applications. Therefore, we used green synthesized ZnO nanoparticles to fabricate dye-sensitized solar cells (DSSC). From the J-V curves, we calculated the DSSC parameters such as open-circuit voltage (V_{oc}), short circuit current density (J_{sc}), fill factor (FF) and efficiency (η), and their values were 0.65 V, 6.26 mA, 48.5%, and 1.97%, respectively, at 100 mW/cm^2.

1. Introduction

Most of the researchers are preparing different varieties of nanomaterials due to their panoptic range of applications and amazing properties [1–5]. These are especially used in energy applications like photovoltaic cells and electrochemical applications [6–10]. One among them is Zinc oxide (ZnO) nanoparticles; it has attracted the attention of scientists due to its unique optical, electrical and semiconductor properties along with the wide bandgap and large exciton binding energy [11,12]. ZnO nanoparticles are used in dye-sensitized solar cells (DSSC), electrochemical sensors, paint cosmetics industries, gas sensors, photocatalysts, pharmaceuticals, rubber, etc. ZnO nanoparticles are prepared from various methods like chemical precipitation, sol-gel, solution free mechanochemical method, hydrothermal method, etc. These methods are sometimes time consuming and tedious, may require special expensive instrumental setups, toxic chemicals, high temperatures and templates (which may result in impurities). On the other hand, the biological method of preparing ZnO nanoparticles is an easy, eco-friendly, non-toxic, simple and cost-effective method compared to the above methods. The main advantage of this method is the huge availability of different types of plants and the presence of phytochemicals like aldehydes, ketones, flavonoids, and phenols in plants. These phytochemicals act as reducing agents as well as capping agents [13]. Generally, the biological synthesis of metal oxide nanoparticles mainly depends upon the type of solvent used, pH, pressure, temperature, etc. and can be achieved easily [14]. This method is fast, robust and has many advantages over other methods of preparing nanoparticles. Therefore, we report the green synthesis of ZnO nanoparticles by using *Tilia Tomentosa* (Ihlamur) leaves extract.

Ihlamur or Linden is a common plant of Turkey and it belongs to the family of the genus Tilia, generally found in the form of trees or shrubs [15]. These plant leaves and flowers exhibit good aroma and are used extensively to prepare herbal tea in Turkey for centuries. It possesses light yellowish color with soothing features and proved to be very effective against the common cold, fever, headache, sore throat, high blood pressure, etc. They are rich in antioxidants, flavonoids and shows significant antimicrobial activity. Many researchers reported the preparation of ZnO nanoparticles by using

* Corresponding author.
E-mail address: shashankaic@gmail.com (R. Shashanka).
Peer review under responsibility of Vietnam National University, Hanoi.

https://doi.org/10.1016/j.jsamd.2020.04.005

different plant leaves but no one reported the preparation of ZnO nanoparticles by using Ihlamur plant leaves as to our knowledge. Jamdagni et al. [16] prepared ZnO nanoparticles by using Nyctanthes arbor-tristis flower extract and optimized the synthesis conditions for maximal and narrow size particle? range. Bhumi et al. [17] synthesized ZnO nanoparticles from Catharanthus roseus leaf extract and validated them for antibacterial activity. They reported that the biological synthesis of ZnO nanoparticles is a robust, easy, economical and environmentally friendly method.

One more important property of ZnO nanoparticles is their ability to act as a semiconductor due to a wide bandgap. Therefore, we fabricated DSSC using our green synthesized ZnO nanoparticles. O'Regan and Gratzel [18] reported the use of DSSC for the first time and from there on DSSC has emerged as one of the energy-saving inventions of all time. Presently, there is a huge need for clean and renewable energy globally to support our modern society activities. The use of DSSC is the best option to satisfy the need of electric energy by converting solar energy into electric energy directly. The DSSC is one of the conventional methods used to produce electric energy from renewable sources and hence has attracted the attention of many researchers due to their easy fabrication process, low manufacturing cost and eco-friendly nature [19]. ZnO nanoparticles are one of the most promising candidates to fabricate the next-generation DSSC due to their wide bandgap and excellent exciton binding energy at room temperature.

DSSC's using green synthesized photoanode have still not achieved the desired high efficiency. Rathnasamy et al. [20] synthesized hexagonal wurtzite ZnO nanoparticles by a green synthesis method using *Carica papaya* leaf extract. They used the synthesized ZnO nanoparticles as a photoanode in the dye-sensitized solar cell and achieved 1.6% efficiency in energy conversion. Also, Sharma et al. [21] synthesized ZnO nanoparticles from the leaves extract of Calotropis gigantean and used them as photoanodes in dye-sensitive solar cells and achieved 0.66% efficiency.

Many researchers have reported the use of ZnO nanoparticles prepared by chemical and physical methods to fabricate DSSC but very limited literature is reported to use ZnO nanoparticles prepared from biological methods to fabricate DSSC. Therefore, in the present paper, we report a green synthesis of ZnO nanoparticles using *Tilia Tomentosa* (Ihlamur) leaves extract and its potential application in DSSC. Furthermore, it should be emphasized that the obtained efficiency value (1.97%) is higher than that of the reported studies.

2. Experimental

2.1. Chemicals and reagents required

Zinc nitrate hexahydrate [$Zn(NO_3)_2 \cdot 6H_2O$], Sodium hydroxide (NaOH), Triton-X 100 and acetylacetone were purchased from Sigma-Aldrich. The plant extract was prepared in the lab using *Tilia Tomentosa* (Ihlamur) leaves and all the solutions were prepared by using double distilled water.

2.2. Preparation of plant extract

The dried leaves of *Tilia Tomentosa* (Ihlamur) were collected from Bartin, Turkey. The dried leaves were blended carefully in a blender to get uniform powders. Then 10 g of powdered leaves were mixed with 200 mL of deionized water and the solution was boiled at 80 °C for 15 min until a strong yellow colored solution remains. Then the solution was cooled to room temperature and filtered to get a clean yellow colored solution of plant extract. This plant extract acts as both reducing agent as well as capping agent. A small amount of fresh leaf extract is used to prepare ZnO nanoparticles and the remaining will be stored at 5 °C temperature for further use.

2.3. Preparation of ZnO nanoparticles

We prepared a 0.1 M Zinc nitrate hexahydrate solution by dissolving 2.972 g of salt in a 100 mL standard flask using double distilled water. The solution was agitated on a magnetic stirrer for 5 min at room temperature to get a homogenous solution. Then 20 mL of Ihlamur plant extract was added with continuous stirring at 80 °C for 30 min on a magnetic stirrer. The solution turns yellow after adding the plant extract. After 30 min of stirring, 1 M NaOH was added dropwise till the yellow color solution turns into a pale yellow color precipitate. Stirring at 80 °C was continued for 1–2 min for complete precipitation. Next, the solution was cooled to room temperature and the solution was centrifuged for 10 min at an rpm of 7500. The supernatant solution was removed and washed with water and again centrifuged. After 3 times of centrifugation, the pale yellow/white ZnO nanoparticles were collected on a watch glass and dried at 70 °C in an oven overnight. The dried ZnO nanoparticles were calcined in a furnace at 400 °C with a holding time of 15 min to remove any evaporable impurities. The calcined samples were cooled to room temperature and stored it for further characterization. Fig. 1 shows the graphical representation of preparing ZnO nanoparticles using *Tilia Tomentosa* (Ihlamur) leaves extract.

2.4. Fabrication of ZnO based DSSC

ZnO nanopowders were coated onto the fluorine-doped tin oxide (FTO) with a surface area of 0.25 cm^2 using the doctor blade method. For the coating, ZnO nanopowders were mixed with a certain amount of Triton-X 100, acetylacetone and ultrapure water and pestle to obtain a paste. The paste was squeezed on the FTO surface by a razor blade to form a ZnO film. The produced film was subjected to annealing to remove organic residues at 450 °C for 2 h. The annealed film was immersed in 0.5 mM N719 ((cis-diisothiocyanato-bis(2,2′-bipyridyl-4,4′-dicarboxylato) ruthenium (II) bis(-tetrabutylammonium): ruthenizer 535 bis-TBA, Solaronix Co.)) dye solution for 2 h at room temperature at dark and later it was rinsed with methanol and dried. The resulting photoanode was observed to be red-violet. The dye-absorbed ZnO film was clipped with a platinum-coated counter electrode to provide a sandwich-type DSSC formation and the sealed tape was used to prevent short-circuiting. For the final step of DSSC fabrication, the redox electrolyte (Iodolyte AN-50, Solaronix Co.) was injected into the device through the gap in the counter electrode. The structure of ZnO based DSSC is also shown in Fig. 1.

2.5. Characterization of ZnO nanoparticles

The XRD (RIGAKU SmartLab) is used to investigate the phases present in the prepared ZnO nanoparticles at the 2θ range of 20–80° using Cu $Ka_{\alpha 1}$ radiation ($\lambda = 1.54056$ Å). The topographical morphology of the ZnO nanoparticles was investigated by using scanning electron microscopy (SEM) (TESCAN- MAIA3 XMU) and their elemental quantification was performed by energy dispersive spectroscopy (EDS) attached to SEM. The absorption spectra were recorded on the SHIMADZU UV 3600 plus spectrophotometer. Photocurrent-voltage characteristics of the ZnO-DSSC were measured by FYTRONIX OPTOSENSE on a solar simulator under illumination with a power density of AM1.5 (100 mW/cm^2).

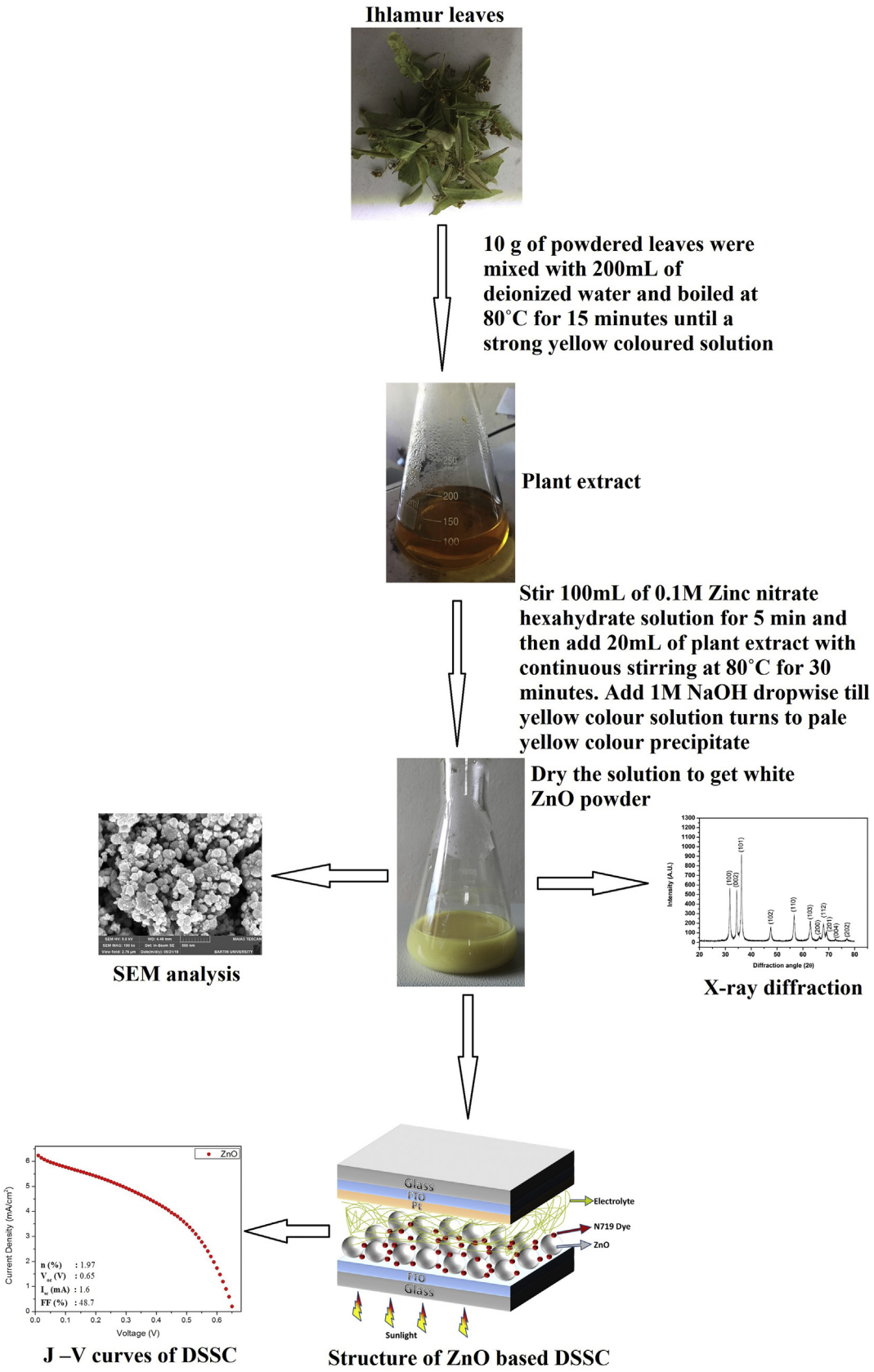

Fig. 1. Graphical representation of the preparation of ZnO nanoparticles using the *Tilia Tomentosa* (Ihlamur) leaves extract.

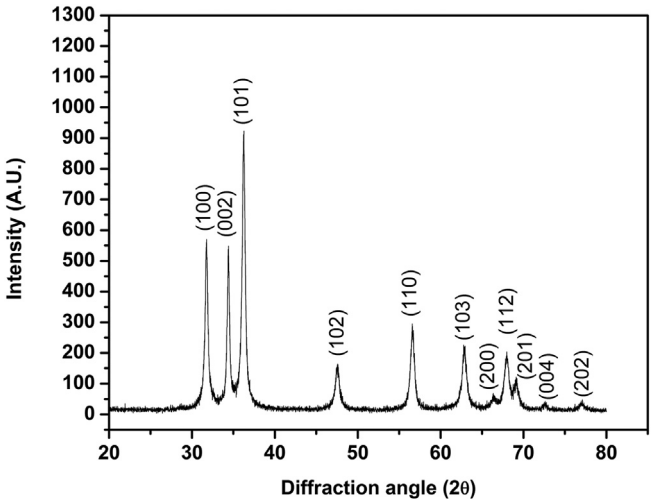

Fig. 2. XRD diffraction pattern of ZnO nanoparticles prepared by *Tilia Tomentosa* (Ihlamur) leaves extract.

3. Results and discussion

3.1. Structural analyses of the ZnO nanoparticles

The X-ray diffraction (XRD) pattern of the prepared ZnO nanoparticles is depicted in Fig. 2. The diffraction peaks at 2θ of 31.71°, 34.37°, and 36.22° correspond to (100), (002) and (101) planes, respectively, and confirms the formation of ZnO (Zincite) with hexagonal structure. All the peaks were well matched with the JCPDF Card No.: 01-076-0704. The diffraction peaks of the prepared ZnO nanoparticles were broadened due to their retained nanostructure even after calcination [22,23]. The peak broadening is also due to high strain, instrumental errors, etc. [24–27]. To calculate the average crystallite size of synthesized ZnO nanoparticles, we used Scherrer's formula [28–30];

$$D = \frac{K\lambda}{\beta \cos\theta} \quad (1)$$

where D is an average crystallite size, K is a constant equal to 0.94, λ is the wavelength of X-ray radiation (0.154 nm), β is Full-width half maximum of the peak (in radians) and 2θ is Bragg's angle (degree). We have calculated the crystallite size for the diffraction peaks (100), (002) and (101) using Scherrer's equation and found the average crystallite size value to be approximately 22 nm. Lattice parameters were found to be a = 3.25 Å, b = 3.25 Å, c = 5.21 Å and lattice angles are $\alpha = 90°$, $\beta = 90°$ and $\gamma = 120°$, respectively. Similarly, the space group of the prepared ZnO nanoparticles was found to be 186:P63mc. The intensities and diffraction peak's positions were well matched with the reported values.

3.2. Scanning electron microscopy analysis of the ZnO nanoparticles

Fig. 3 (a) represents the SEM microstructure of ZnO nanoparticles prepared by *Tilia Tomentosa* (Ihlamur) leaves. The SEM microstructure depicts the spherical nature of the prepared nanoparticles with similar sizes. The average sizes of the spherical ZnO nanoparticles were found to be about 80 nm. The prepared ZnO nanoparticles are homogeneous in nature with little agglomeration because of their very fine size. We have not used expensive and toxic capping agents to reduce agglomeration but, the plant extract itself acts as both reducing agent and capping agent. Therefore, this method is more economical and eco-friendly than any other method of preparing ZnO nanoparticles.

Fig. 3 (b) shows the EDS image of ZnO nanoparticles prepared by Ihlamur plant extract. The EDS analysis was performed to study the composition of elements present in the ZnO nanoparticles. The atomic percentage of zinc and oxygen was calculated theoretically and the value was found to be 50% each. Similarly, the atomic percentage of zinc and oxygen was determined experimentally and the values were found to be 50% each. As we have seen from the EDS data, both zinc and oxygen atoms present in prepared ZnO nanoparticles are stoichiometric to each other and are agree with the theoretical values.

3.3. Optical characterization of the ZnO

UV-vis spectroscopy was used to study the optical band gap of ZnO nanoparticles. The prepared ZnO nanoparticles were dispersed uniformly in deionized water using an ultra sonicator for 2 min to get a homogeneous solution. Fig. 4 shows the UV-visible spectrum of green synthesized ZnO nanoparticles. The spectrum shows a broad absorption peak at 350 nm which is due to the surface plasmon absorption of ZnO nanoparticles. This surface plasmon

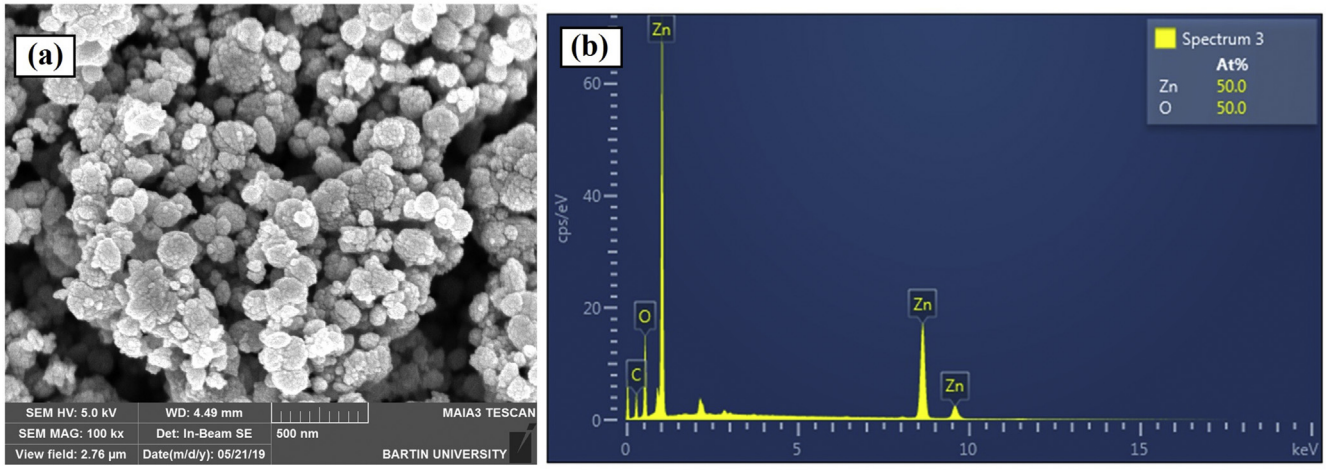

Fig. 3. **(a)** SEM image and **(b)** Energy dispersive spectroscopy (EDS) image of the synthesized ZnO nanoparticles.

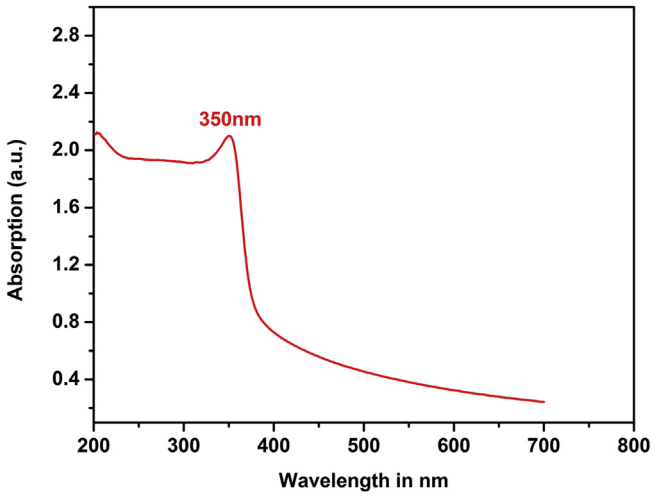

Fig. 4. UV-Visible spectrum of the green synthesized ZnO nanoparticles.

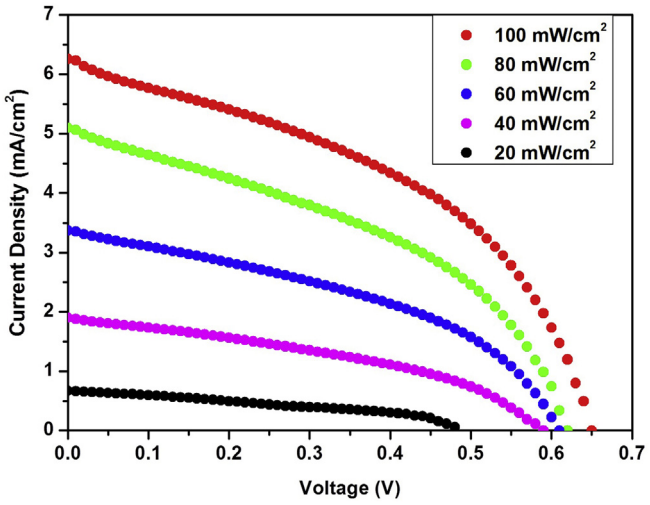

Fig. 5. *J* –*V* curves of ZnO-DSSC at different light intensities.

absorption phenomenon occurs due to the collective oscillation of the free conduction band electrons when electromagnetic radiation strikes them [31,32]. The UV-Visible absorption peak obtained for ZnO nanoparticles in the present study is comparable with other reports.

The bandgap energy (E) of prepared ZnO nanoparticles were calculated by using the following equation [32]:

$$E = \frac{h \times C}{\lambda} \quad (2)$$

where E = Bandgap energy
h = Planks constant = 6.626×10^{-34} J s.
C = Speed of light = 3.0×10^{8} m/s
λ = Cut off wavelength = 350×10^{-9} m.
*Conversion 1eV = 1.6×10^{-19} J.

The calculated band gap energy value was found to be 3.55 eV and this intrinsic bandgap absorption of ZnO is due to the electron transitions from the valence band to the conduction band. Due to the absorption of ZnO nanoparticles at the UV region, they can be used in medical applications such as sunscreen protectors or as antiseptic ointments [32].

3.4. Electrical characterization of ZnO based DSSC

The fill factor of DSSC can be calculated by:

$$FF = \frac{J_{max} \times V_{max}}{J_{SC} \times V_{OC}} \quad (3)$$

where J_{max}, V_{max}, *JSC*, *VOC* are the values of the current density and the voltage for the maximum power point, short current density (*JSC*) of the measured current at 0 V, and the open-circuit voltage (*VOC*), respectively. The power conversion efficiency (*n%*), which is the ratio between maximum power (*Pmax*) and electrical input power (*Pin*), is calculated by the following equation:

$$n = \frac{FF \times V_{OC} x J_{SC}}{S x P_{in}} \quad (4)$$

where S is the area of the DSSC [33].

The current density-voltage (*J-V*) curve of the ZnO based DSSC at different light intensities is shown in Fig. 5. From the *J-V* curves, the DSSC parameters such as open-circuit voltage (V_{oc}), short circuit current density (J_{sc}), fill factor (*FF*) and efficiency (η) were

Table 1
The photovoltaic parameters of ZnO-DSSCs.

Lighting Intensity (mW/cm^2)	J_{sc} (mA/cm2)	V_{oc} (V)	*n* (%)	*FF* (%)
20	0.67	0.49	1.01	61.3
40	1.90	0.59	1.11	35.9
60	3.37	0.61	1.41	41.3
80	5.10	0.62	1.65	41.6
100	6.26	0.65	1.97	48.5

calculated using Equations (3) and (4). The calculated values of the DSSC parameters are given in Table 1. The *n%* value of the fabricated ZnO based DSSC was found to be quite good compared to the studies with similar ZnO nanoparticle structures in the literature [34]. It has been reported that the dipping time of a ZnO film into a sensitizing dye is a key factor for solar cell parameters of the ZnO-based DSSC [35]. The produced ZnO-based DSSC achieved higher efficiency in a shorter period of dipping time compared to similar studies [20]. The high efficiency can also be explained by the increased absorption due to the increase in the number of dye molecules adsorbed onto the ZnO surface. Therefore, because the method is simple and the samples can easily be prepared, the use of ZnO nanoparticles in photovoltaics is promising for the future. The current density value was found to be relatively low. The most important parameter that determines the overall efficiency limit of the system is the photocurrent. If the particle size approaches to the nano level, then parental materials behave differently due to their high surface area and surface energy [36–38]. The average crystallite size of the prepared ZnO nanoparticles is found to be about 22 nm. Therefore, we can expect significant photochemical properties. Various factors such as a small roughness factor, reflection or scattering in the photoanode, low injection efficiency, charge collection efficiency can cause a relatively low photocurrent [39]. As the light intensity increased, the short circuit current value linearly increased to the values close to saturation. The linear increase in (J_{sc}) was attributed to higher photogenerated excitons [40]. Therefore, more electron densities were transferred to ZnO at higher light intensities. It can be seen from Table 1 that the *n* and J_{sc} values increased as the applied light density rises. An increase in light intensity is attributed to an increase in charge generation. Similar observations have been reported for the ZnO-based DSSC [35]. These results show that when the intensity of illumination is increased up to 100 mW/cm^2, there is no significant change in transport, injection and recombination mechanisms.

4. Conclusion

The ZnO nanoparticles were successfully prepared by an easy and eco-friendly plant-mediated biological method using leaves of *Tilia Tomentosa* (Ihlamur). The synthesized ZnO nanoparticles showed a single-phase hexagonal structure with an average crystallite size of 22 nm as calculated from Scherrer's equation. SEM study unveiled the spherical nature of the nanoparticles with little agglomeration. In the present experiment, we have not used any extra capping agents to reduce agglomeration due to their toxic nature; but, the plant extract itself acts as both a reducing agent as well as a capping agent. Therefore, the present method is more economical and eco-friendly than other methods for preparing ZnO nanoparticles. The average particle size of the ZnO nanoparticles was found to be 80 nm. The EDS analysis confirmed the 1:1 stoichiometric ratio of zinc and oxygen, both theoretically and experimentally. The UV-Visible spectroscopy of the ZnO nanoparticles showed a broad surface Plasmon resonance absorption peak at 350 nm with a bandgap of 3.55eV. The ZnO nanoparticle-based DSSC was successfully fabricated and their performance was investigated from the current density-voltage behavior under simulated sunlight. The high efficiency of the fabricated DSSC is due to a significant increase in the absorption of dye molecules onto the surface of ZnO nanoparticles. Therefore, the use of green synthesized ZnO nanoparticles in fabricating DSSC is an easy and promising method for the wellness of our future.

Declaration of Competing Interest

The authors declare that they have no known competing financial interests or personal relationships that could have appeared to influence the work reported in this paper. Overall, there is no conflict of interest.

Acknowledgments

The authors gratefully acknowledge Bartin University Scientific Research Projects Unit, Turkey for providing financial support to conduct the research (Project number: 2019-FEN-A-006).

References

[1] J.G. Manjunatha, Electroanalysis of estriol hormone using electrochemical sensor, Sens. Bio-Sens. Res. 16 (2017) 79–84.
[2] J.G. Manjunatha, M. Deraman, N.H. Basri, I.A. Talib, Fabrication of poly (Solid Red A) modified carbon nano tube paste electrode and its application for simultaneous determination of epinephrine, uric acid and ascorbic acid, Arabian J. Chem. 11 (2018) 149–158.
[3] J.G. Manjunatha, M. Deraman, N.H. Basri, N.S.M. Nor, I.A. Talib, N. Ataollahi, Sodium dodecyl sulfate modified carbon nanotubes paste electrode as a novel sensor for the simultaneous determination of dopamine, ascorbic acid, and uric acid, Compt. Rendus Chem. 17 (2014) 465–476.
[4] J.G. Manjunatha, A novel poly (glycine) biosensor towards the detection of indigo carmine: a voltammetric study, J. Food Drug Anal. 26 (2018) 292–299.
[5] G. Tigari, J.G. Manjunatha, Electrochemical preparation of poly(arginine)-modified carbon nanotube paste electrode and its application for the determination of pyridoxine in the presence of riboflavin: an electroanalytical approach, J. Anal. Test. 3 (2019) 331–340.
[6] C. Raril, J.G. Manjunatha, A simple approach for the electrochemical determination of vanillin at ionic surfactant modified graphene paste electrode, Microchem. J. 154 (2020) 104575.
[7] G. Tigari, J.G. Manjunatha, C. Raril, N. Hareesha, Determination of riboflavin at carbon nanotube paste electrodes modified with an anionic surfactant, ChemistrySelect 4 (2019) 2168–2173.
[8] N. Hareesha, J.G. Manjunatha, C. Raril, G. Tigari, Sensitive and selective electrochemical resolution of tyrosine with ascorbic acid through the development of electropolymerized alizarin Sodium sulfonate modified carbon nanotube paste electrodes, ChemistrySelect 4 (2019) 4559–4567.
[9] P.A. Pushpanjali, J.G. Manjunatha, M.T. Shreenivas, The electrochemical resolution of ciprofloxacin, riboflavin and estriol using anionic surfactant and polymer-modified carbon paste electrode, ChemistrySelect 4 (2019) 13427–13433.
[10] G. Tigari, J.G. Manjunatha, A surfactant enhanced novel pencil graphite and carbon nanotube composite paste material as an effective electrochemical sensor for determination of riboflavin, J. Sci.: Adv. Mater. Dev. 5 (2020) 56–64.
[11] Q. Ahsanulhaq, A. Umar, Y.B. Hahn, Growth of aligned ZnO nanorods and nanopencils on ZnO/Si in aqueous solution: growth mechanism and structural and optical properties, Nanotechnology 18 (2007) 115603.
[12] S. Reddy, B.E. Kumara Swamy, S. Aruna, M. Kumar, R. Shashanka, H. Jayadevappa, Preparation of NiO/ZnO hybrid nanoparticles for electrochemical sensing of dopamine and uric acid, Chem. Sensor. 2 (2012) 1–7.
[13] M. Doble, A.K. Kruthiventi, Green Chemistry and Engineering, first ed., Academic Press, 2007.
[14] J. Singh, T. Dutta, K.-H. Kim, M. Rawat, P. Samddar, P. Kumar, Green synthesis of metals and their oxide nanoparticles: applications for environmental remediation, J. Nanobiotechnol. 16 (2018) 1–24.
[15] D. McCarthy, Systematics and Phylogeography of the Genus Tilia in North America, Ph.D. dissertation, University of Illinois, Chicago. Pigott, D, 2012.
[16] P. Jamdagni, P. Khatri, J.S. Rana, Green synthesis of zinc oxide nanoparticles using flower extract of Nyctanthes arbor-tristis and their antifungal activity, J. King Saud Univ. Sci. 30 (2018) 168–175.
[17] G. Bhumi, N. Savithramma, Biological Synthesis of Zinc oxide Nanoparticles from Catharanthus roseus (l.) G. Don. Leaf extract and validation for antibacterial activity, Int. J. Drug Dev. Res. 6 (2014) 208–214.
[18] B. O'Regan, M. Grätzel, A low-cost, high-efficiency solar cell based on dye sensitized colloidal TiO_2 films, Nature 353 (1991) 737–740.
[19] F. Shao, J. Sun, L. Gao, S. Yang, J. Luo, Growth of various TiO_2 nanostructures for dye-sensitized solar cells, J. Phys. Chem. C 115 (2011) 1819–1823.
[20] R. Rathnasamy, P. Thangasamy, R. Thangamuthu, S. Sampath, V. Alagan, Green synthesis of ZnO nanoparticles using Carica papaya leaf extracts for photocatalytic and photovoltaic applications, J. Mater. Sci. Mater. Electron. 28 (2017) 10374–10381.
[21] J.K. Sharma, P. Srivastava, G. Singh, M.S. Akhtar, S. Ameen, Green synthesis of Co_3O_4 nanoparticles and their applications in thermal decomposition of ammonium perchlorate and dye-sensitized solar cells, Mater. Sci. Eng., B 193 (2015) 181–188.
[22] R. Shashanka, D. Chaira, Development of nano-structured duplex and ferritic stainless steel by pulverisette planetary milling followed by pressureless sintering, Mater. Char. 99 (2015) 220–229.
[23] R. Shashanka, D. Chaira, Optimization of milling parameters for the synthesis of nano-structured duplex and ferritic stainless steel powders by high energy planetary milling, Powder Technol. 278 (2015) 35–45.
[24] R. Shashanka, D. Chaira, B.E.K. Swamy, Electrocatalytic response of duplex and yittria dispersed duplex stainless steel modified carbon paste electrode in detecting folic acid using cyclic voltammetry, Int. J. Electrochem. Sci. 10 (2015) 5586–5598.
[25] A.K. Nayak, R. Shashanka, D. Chaira, Effect of nanosize yittria and tungsten addition to duplex stainless steel during high energy planetary milling, IOP Conf. Ser. Mater. Sci. Eng. 115 (2016) 12008.
[26] S. Gupta, R. Shashanka, D. Chaira, Synthesis of nano-structured duplex and ferritic stainless steel powders by planetary milling: an experimental and simulation study, IOP Conf. Ser. Mater. Sci. Eng. 75 (2015) 12033.
[27] R. Shashanka, Synthesis of nano-structured stainless steel powder by mechanical alloying-an overview, Int. J. Sci. Eng. Res. 8 (2017) 588–594.
[28] R. Shashanka, D. Chaira, B.E.K. Swamy, Fabrication of yttria dispersed duplex stainless steel electrode to determine dopamine, ascorbic and uric acid electrochemically by using cyclic voltammetry, Int. J. Sci. Eng. Res. 7 (2016) 1275–1285.
[29] R. Shashanka, D. Chaira, B.E.K. Swamy, Electrochemical investigation of duplex stainless steel at carbon paste electrode and its application to the detection of dopamine, ascorbic and uric acid, Int. J. Sci. Eng. Res. 6 (2015) 1863–1871.
[30] R. Shashanka, D. Chaira, Phase transformation and microstructure study of nano-structured austenitic and ferritic stainless steel powders prepared by planetary milling, Powder Technol. 259 (2014) 125–136.
[31] R. Shashanka, B.E.K. Swamy, Biosynthesis of silver nanoparticles using leaves of Acacia melanoxylon and its application as dopamine and hydrogen peroxide sensors, Phy. Chem. Res. 8 (1) (2020) 1–18.
[32] R. Shashanka, Y. Kamacı, R. Taş, Y. Ceylan, A.S. Bülbül, O. Uzun, A.C. Karaoglanli, Antimicrobial investigation of CuO and ZnO nanoparticles prepared by a rapid combustion method, Phy. Chem. Res. 7 (4) (2019) 799–812.
[33] Q. Zhang, C.S. Dandeneau, X. Zhou, G. Cao, ZnO nanostructures for dye-sensitized solar cells, Adv. Mater. 21 (41) (2009) 4087–4108.
[34] A.E. Suliman, Y. Tang, L. Xu, Preparation of ZnO nanoparticles and nanosheets and their application to dye-sensitized solar cells, Sol. Energy Mater. Sol. Cell. 91 (18) (2007) 1658–1662.
[35] E. Guillén, F. Casanueva, J.A. Anta, A. Vega-Poot, G. Oskam, R. Alcántara, C. Fernández-Lorenzo, J. Martín-Calleja, Photovoltaic performance of

nanostructured zinc oxide sensitised with xanthene dyes, J. Photochem. Photobiol. Chem. 200 (2–3) (2008) 364–370.
[36] R. Shashanka, B.E.K. Swamy, S. Reddy, D. Chaira, Synthesis of silver nanoparticles and their applications, Anal. Bioanal. Electrochem. 5 (2013) 455–466.
[37] R. Shashanka, Effect of sintering temperature on the pitting corrosion of ball milled duplex stainless steel by using linear sweep voltammetry, Anal. Bioanal. Electrochem. 10 (2018) 349–361.
[38] R. Shashanka, Non-lubricated dry sliding wear behavior of spark plasma sintered nano-structured stainless steel, J. Mater. Environ. Sci. 10 (8) (2019) 767–777.
[39] A.B.F. Martinson, J.W. Elam, J.T. Hupp, M.J. Pellin, ZnO nanotube based dye-sensitized solar cells, Nano Lett. 7 (8) (2007) 2183–2187.
[40] B. Pradhan, S.K. Batabyal, A.J. Pal, Vertically aligned ZnO nanowire arrays in Rose Bengal-based dye-sensitized solar cells, Sol. Energy Mater. Sol. Cell. 91 (9) (2007) 769–773.